Synthesis and Coordination of a Bisphosphine-[NHC-borane] Compound: A Ligand Framework for Bimetallic Structure Featuring a Boron-Bridging Moiety

Aurèle Camy, Laure Vendier, Christian Bijani, Israel Fernández, Sébastien Bontemps

Synthesis and coordination of a bisphosphine-[NHC-borane] compound: a ligand framework for bimetallic structure featuring a boron-bridging moiety

Aurèle Camy,[a] Laure Vendier,[a] Christian Bijani,[a] Israel Fernández[b] and Sébastien Bontemps*[a]*

[a]LCC-CNRS, Université de Toulouse, CNRS, 205 route de Narbonne, 31077 Toulouse Cedex 04, France

[b] Departamento de Química Orgánica I and Centro de Innovación en Química Avanzada (ORFEO—CINQA), Facultad de Ciencias Químicas, Universidad Complutense de Madrid 28040 Madrid (Spain)

ABSTRACT. We report herein the synthesis of a bisphosphine-[NHC-BH_3] compound and its coordination to gold. The ligand is shown to support a bimetallic structure bisphosphine-[NHC-BH_3]$(AuCl)_2$. The abstraction of one chloride from the gold metal center triggers the activation of the BH_3 fragment leading to the reductive elimination of H_2 and the formation of a dicationic Au_4^{2+} complex featuring Au centers at the +0.5 oxidation state, via a (μ-H)Au_2 intermediate, characterized *in situ* at 183 K. The reactivity of the Au_4 with thiophenol led to the re-oxidation of the gold metal centers to a (μ-S(Ph))Au_2 complex. In the different complexes, the borane moiety was shown to bridge Au_2 core via weak interaction with [BH], [BCl] and [BH_2] moieties.

INTRODUCTION

In the field of ligand design, elegant strategies were developed for the preparation of bimetallic structures.[1-8] Defined molecular multimetallic systems are indeed of high interest to understand and eventually emulate the activity of polymetallic enzymatic or heterogeneous catalysts. In some cases, the ligand framework supporting bimetallic structures incorporates one moiety bridging the two metal centres.[9-13] This feature serves both as a structuring site and also as an additional reactive center. O, S, N and C atoms are usual bridging elements, found either in metalloenzymes[14-18] and/or in heterogeneous catalysts (Chart 1a).[19-20]

Although boron is not known to be a bridging element in metalloenzymes, it constitutes a specific and powerful doping agent in various energy materials, notably because of its p-dopant properties.[21-23] We thus believe that developing ligand frameworks supporting bimetallic systems with boron-containing bridging fragments at the molecular level is important (Chart 1a). Moreover, the very versatile behavior of this element in the vicinity of transition metals[24] – as borate (coordinated or not),[25-27] Z-type borane,[28-32] boryl,[33-34] and terminal or bridging borylene[35-36] – should offer a very broad scope of coordination modes in bimetallic systems. To the best of our knowledge, however, only bisphosphine-boryl ligands – initially developed by Yamashita, Nozaki *et al*. as pincer ligands for mononuclear complexes[37-39] - were shown to support bimetallic structures of Ni and Co[12] and recently of Cu.[9] Interestingly, the bimetallic Ni and Co complexes were shown to reversibly react with H_2 via bifunctional activation between the metal centers and the boron-containing moiety, which alternated between boryl and hydroborane forms.

In this context, we aimed at designing a ligand framework that would support a bimetallic structure *and* feature a central bridging boron-containing moiety (Chart 1b). We selected NHC-borane as the central moiety of the ligand – because of the known ability of carbene to stabilize various boron-containing species[40-41] – with two adjacent phosphine buttresses. We expected to stabilize

the coordination of the central NHC-borane moiety with adjacent phosphine buttresses to expand the coordination chemistry of carbene-borane compounds. Compared to the wealth of reports of organic and main group chemistry of carbene-borane,[40-41] the coordination chemistry of unsupported carbene-borane is indeed limited to the following examples: i) NHC-BH_3 were shown to weakly bind Mn, Cr, Mo and W metal centres,[42] ii) a B-H bond was activated at Fe and W alkyl precursors,[43-44] iii) NHC-haloborane led to a very original NHC-borido Co complex[45] and finally iii) the coordination of carbene-cyanoboryl generated three carbene-boryl Au complexes.[46-48]

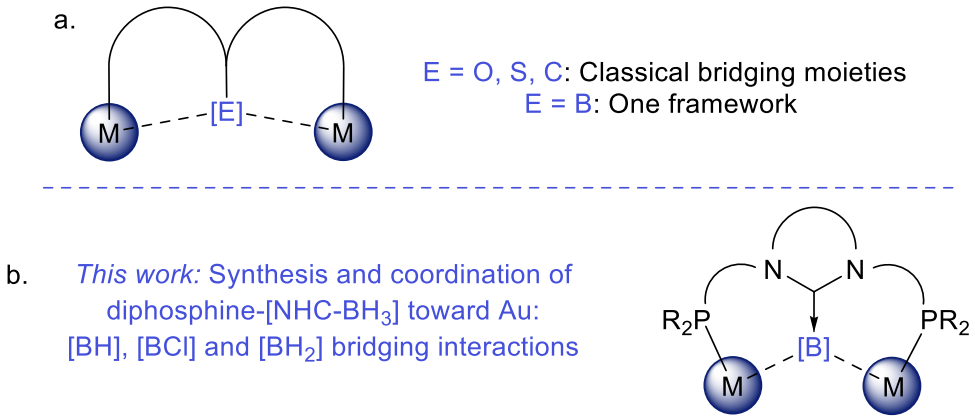

Chart 1. a) Classical bridging moieties in bimetallic complexes, b) Highlights of this work

Herein we present the synthesis of the first compound of this type and its coordination toward gold. As it will be described, the synthesized bisphosphine-[carbene-borane] is able to support bimetallic structures. Interestingly, upon chlorine abstraction from Au(I), the BH_3 fragment is involved in reductive elimination of H_2 at gold leading to the isolation of a Au_4 cluster. The formation of the cluster, its bonding description and its reactivity toward thiol were studied by experimental and theoretical means. Particular attention was paid to the versatile coordination behavior of the borane fragment as a central bridging moiety.

RESULTS AND DISCUSSION

The bisphosphine-benzimidazolium compound **1** (Scheme 1) was synthesized according to the literature procedure in five steps with an overall yield of 40%.[49-50] In toluene, the addition of KHMDS at room temperature followed by Me_3N-BH_3 at 90 °C to compound **1**, led to the generation of compound **2**. In these optimized conditions, compound **2** was isolated in 83% yield on a 3-gram scale (Scheme 1). It is characterized in tol-d_8 by a sharp singlet at 16.6 ppm in $^{31}P\{^1H\}$ NMR and a quartet at -34.1 ppm ($^1J_{B\text{-}H}$ = 89 Hz) in ^{11}B NMR analyses. The hydride signal, integrating for three hydrogen atoms, appears as a singlet at 2.13 ppm in $^1H\{^{11}B\}$ NMR analysis. The carbenic carbon linked to BH_3 is characterized by a broad signal at 183.3 ppm in $^{13}C\{^1H\}$ analysis, at the upper limit of the large range (153.3-186.0 ppm) established by Curran *et al.* from an exhaustive literature survey of carbene-borane compounds.[40]

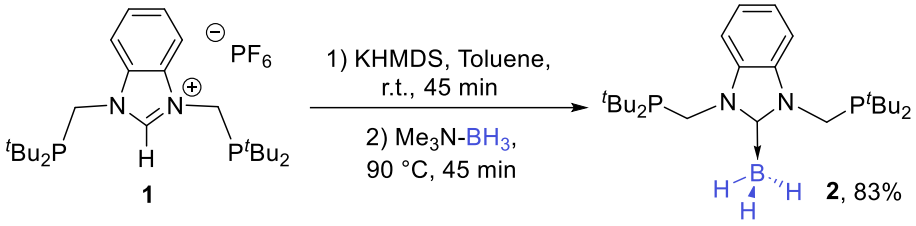

Scheme 1. Synthesis of compound **2**.

Single crystals suitable for X-Ray diffraction (XRD) analysis were obtained from a concentrated pentane solution (Figure 1a). The compound crystallized in the triclinic space group P-1 with six molecules exhibiting very similar features in the asymmetric unit (Figure S97).[51] As shown in Figure 1a, two dihydrogen bonds[52] are detected with [C–H···H–B] distances of 2.08 and 2.15 Å, shorter than the sum of Van der Waals radii of 2.65 Å.[53] While these types of weak hydrogen interactions have been mostly detected with metal hydride as the H-bond acceptor,[54] dihydrogen interaction [C–H···H–B] were reported intramolecularly with azolylborane adducts[53] and intermolecularly with NHC-BH_3 compounds.[55] In both cases, the reported hydridic-protic distances are marginally longer than that found in **2** (2.22 and 2.24 Å for the shortest, respectively),

while the reported intermolecular [N–H···H–B] distances of 2.02 Å are significantly shorter in NH_3-BH_3.[56]

The proximity between the hydrogen atoms of methylene and borane moieties was also observed in solution by NMR spectroscopy. Nuclear Overhauser Effects (NOE) were indeed detected between these nuclei by $^1H/^1H$ NOESY experiment at 298 K in tol-d_8 (Figure S11-12) and the non-equivalence of the methylenic proton was hypothesized based on the broadening of the associated doublet at 4.81 (d, $^2J_{P\text{-}H}$ = 2.6 Hz) at 173 K (Figure S13).

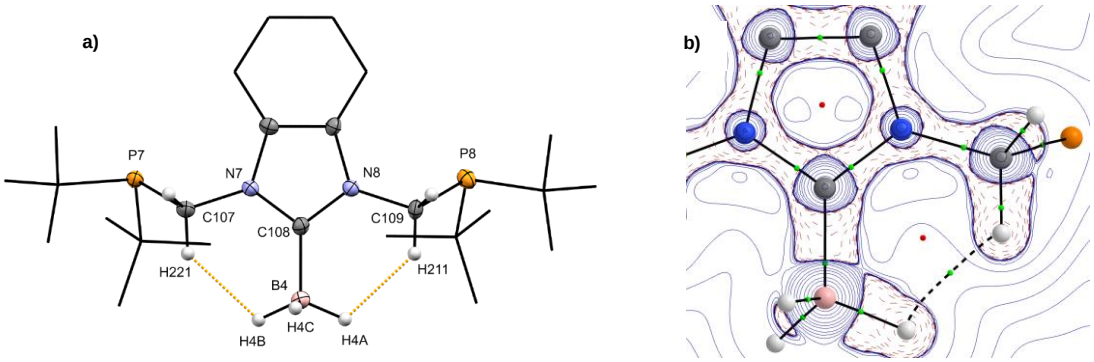

Figure 1. a) Structure of compound **2**. Thermal ellipsoids drawn at 30% probability. Hydrogen atoms are omitted for clarity except in BH_3 and CH_2 moieties which were located in the difference Fourier map and refined freely without any constraint. Selected bond lengths [Å] and angles [°]: C108-B4 1.604(5), B4-H41 1.121(4), B4-H42 1.107(4), B4-H43 1.105(4), H41···H10L 2.085, H42···H10K 2.150, B4-H41-H10L 109.2, C107-H10K-H42 129.8, B4-H42-H10K 106.1, C109-H10L-H41 131.5; **b)** Contour map of Laplacian function ($\nabla^2\rho$) of compound **2** with relevant bond paths (black dashed line) and Bond Critical Points (BCPs, green spheres).

These interactions were characterized by Density Functional Theory (DFT) calculations by having an electrostatic ([B]H and H[C] natural charges of -0.10 and +0.28, respectively) and also a covalent contribution. The latter is observed in the Contour map of Laplacian function by the

occurrence of a Bond Critical Point (BCP) and a Bond Path (BP) running between the two hydrogen atoms (Figure 1b) and described in the NBO analysis as the donation from the doubly-occupied σ(B–H) molecular orbital (MO) to the empty σ*(C–H) MO, with a stabilization energy value of -2.4 kcal/mol.

With compound **2** in hands, we were eager to probe its ability to support bimetallic structure and to observe the role that the central NHC-BH_3 fragment would play. Compound **2** was thus reacted with two equivalents of $AuCl(SMe_2)$ in THF, producing the bimetallic gold(I) complex **3**, isolated in 83% yield (Scheme 2). This compound is characterized by one singlet at 63.6 ppm in $^{31}P\{^1H\}$ NMR analysis, indicative of the coordination of both phosphine moieties. Satisfyingly, the BH_3 fragment is retained upon coordination, as indicated by a well-defined quartet at -33.7 ppm in ^{11}B NMR analysis. The chemical shift of the carbenic carbon at 184.2 ppm is very close to the signal of the starting compound **2**.

X-Ray diffraction analysis showed that the complex crystallized in orthorhombic space group $Pna2_1$ with two molecules in the asymmetric unit of identical geometry. This solid-state analysis confirms the formation of a di-gold complex. The phosphines are linearly coordinated to the Au-Cl fragments (P1-Au1-Cl1 176.82(15)°, P2-Au2-Cl2 173.52(12)°) and these P-Au-Cl segments are both pointing to the same direction, while the central NHC-BH_3 fragment is oriented at the opposite (Figure 2). As in ligand **2**, short hydrogen contacts between the methylene and the borane moieties are observed in the solid-state (2.2, 2.2 and 2.6 Å) as well as in solution, as evidenced by cross-peaks in $^1H/^1H$ NOESY experiment at 298 K in CD_2Cl_2 (Figures S26).

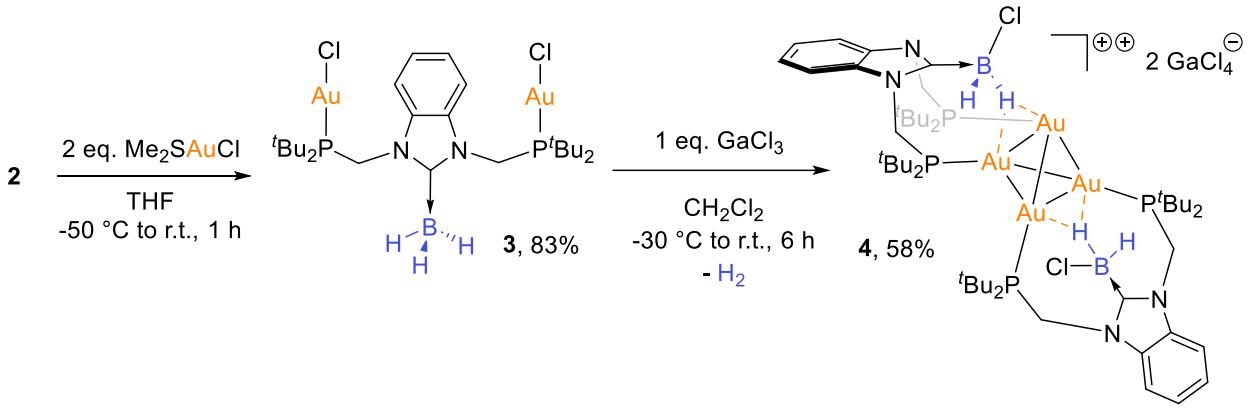

Scheme 2. Synthesis of compounds **3** and **4**.

Complex **3** was reacted with different chloride abstractors.[57] Optimized reaction conditions were found with the addition of 1 equivalent of $GaCl_3$ at low temperature leading to the very clean formation of complex **4**, isolated in 58% yield. Complex **4** is characterized at 243 K in CD_3CN by two triplets in $^{31}P\{^1H\}$ NMR spectrum at 122.9 and 119.0 ppm ($^3J_{P\text{-}P}$ = 23.1 Hz, $^3J_{P\text{-}P}$ = 24.6 Hz), suggesting a AA'BB' system. The formation of a cluster of gold atoms was hypothesized to account for i) the presence of four phosphorus nuclei coupling through metal centers and ii) the large phosphorus deshielding compared to the signal of complex **3** (δP = 63.6) suggesting a change at the metal center. Of note is the characterization of the carbenic carbon at 173.8 ppm in $^{13}C\{^1H\}$ NMR spectrum, almost 10 ppm high-field shifted compared to complex **3**.

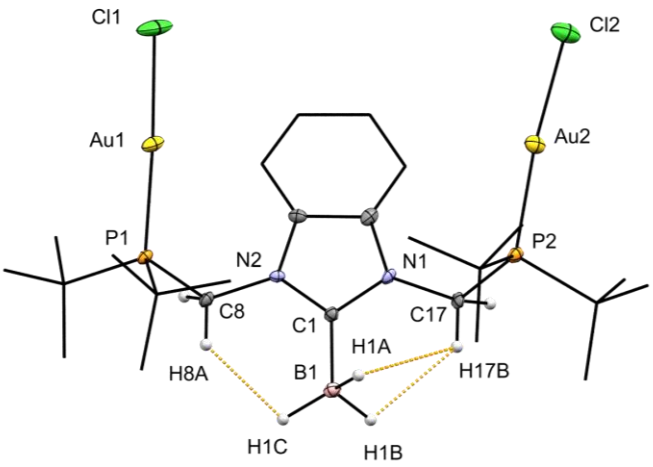

Figure 2. Structure of compound **3**. Thermal ellipsoids drawn at 30% probability. Co-crystallized CH_2Cl_2 and hydrogen atoms are omitted for clarity except in the BH_3 and CH_2 moieties which were located in the difference Fourier map and refined freely without any constraint. Selected bond lengths [Å] and angles [°]: B1-C1 1.607(16), B1-H1A 1.09(3), B1-H1B 1.09(12), B1-H1C 1.13(12), H1A···H17B 2.6, H1B···H17B 2.2, H1C···H8A 2.2, Au1-P1 2.230(3), Au2-P2 2.231(3), Au1-Cl1 2.288(3), Au2-Cl2 2.284(3), P1-Au1-Cl1 176.82(15), P2-Au2-Cl2 173.52(12), C17-H17B-H1A 107, B1-H1B-H17B 102, C17-H17B-H1B 132, B1-H1C-H8A 106, C8-H8A-H1C 135.

XRD analysis showed that complex **4** is a dicationic Au_4 cluster stabilized by two ligands, which crystallized in a triclinic space group P-1 with one molecule in the asymmetric unit (Figure 3). Two bisphosphine-NHC-borane ligands bridge the Au atoms with a single phosphine moiety per Au and four similar P–Au bond lengths (2.287(3) to 2.290(3) Å). The four Au atoms adopt a nearly tetrahedral geometry (Au-Au-Au angles from 59.408(16) to 60.484(16)°). Although Au_4 clusters are rare in Au cluster chemistry,[58-64] the T_d geometry is the usual arrangement adopted by these dicationic species. The Au–Au distances are measured in a narrow range of 2.6979(6) to 2.7274(7)

Å and are rather similar to those in the only two other examples $[R_3PAu]_4^{2+}$ reported to date with P^tBu_3 and $PMes_3$.[62-63] While these 50 valence electrons complexes were not synthesized from the P-Au-X precursors, related $[R_3PAu]_4X_2^{2+}$ complexes (R = aryl, X = halogen) were synthesized from the addition of half an equivalent of a halogen abstractor as in the synthesis of complex **4**.[59]

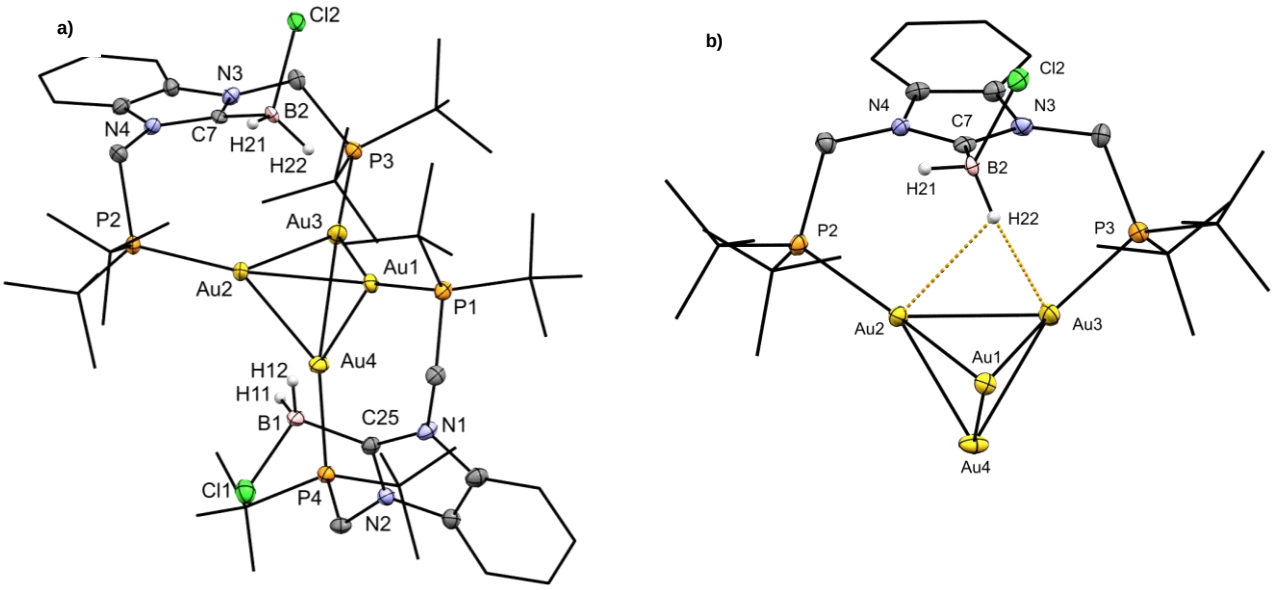

Figure 3. Full (**a**) and partial (**b**) structure of compound **4**. Thermal ellipsoids drawn at 30% probability. The two $GaCl_4$ anions and hydrogen atoms are omitted for clarity, except hydrides on boron which were located in the difference Fourier map and refined with some constraints on distances and angles. Because of these constraints, no esd are provided for bond and angles associated with H atoms. Selected bond lengths [Å] and angles [°]: C7-B2 1.613(15), C25-B1 1.643(18), B2-H22 0.969, B2-H21 0.962, B2-Cl2 1.939(12), B1-H12 0.945, B1-H11 0.949, B1-Cl1 1.898(16), H11-Au4 2.549, H11-Au1 3.058, H22-Au3 2.583, H22-Au2 2.979.

Of note, the borane moiety was modified during the reaction, since the borane is not a BH_3 anymore but a BH_2Cl unit. The central borane participates in the coordination because for each ligand, a B–H bond points toward a Au–Au bond. Although short Au–H distances within the sum of van der Waals radii (2.86 Å) are observed (Figure 3b),[65] the residual density around the cluster

could not be completely resolved (see ESI for details). We thus turned to theoretical calculations to further discuss the nature – if any – of the [BH] interaction in complex **4**. B–H···Au interactions have indeed been observed in few systems with either tris(mercaptoimidazolyl)borate or carbaborane ligands, but not investigated further.[66-70] The geometry of the cluster **4** was well reproduced by DFT. Any attempt to incorporate two hydrogen atoms into the Au_4 cluster did not lead to a minimum. This confirms the loss of one hydrogen atom per ligand in agreement with the detection of dihydrogen by ^{1}H NMR analysis accounting for the reduction of the Au centers (Figure S91). Our calculations show that in complex **4**, the four metal centers behave very similarly with nearly identical bond orders (QTAIM Au-Au delocalization index of ca. 0.37) and electronic charges (ranging from +0.11 to +0.22), in line with a +0.5 oxidation state for each Au metal center as calculated by Pyykkö *et al.* on the parent $[AuPH_3]_4^{2+}$ complex.[71] To gain quantitative insight into the bonding between the cluster and the ligand, the Energy Decomposition Analysis (EDA)–Natural Orbitals for Chemical Valence (NOCV) method was employed. Using $[P_2(NHC\text{-}BH_2Cl)Au_4]^{2+}$ and $P_2(NHC\text{-}BH_2Cl)$ ligand as fragments, the computed total interaction energy (ΔE_{int} = -187.2 kcal/mol) indicates a rather strong bonding, which is mainly dominated by the electrostatic attractions (ΔE_{elstat} = -340.8 kcal/mol) and, to a lesser extent, also by orbital interactions (ΔE_{orb} = -185.5 kcal/mol). The contribution from dispersion forces (ΔE_{disp} = -55.6 kcal/mol) is comparatively weaker, yet not negligible.

The interaction of the central BH_2Cl moieties with the Au cluster was then evaluated. According to the NCIPlot method, there exists a stabilizing non-covalent interaction between the BH fragments and the Au_4 cluster (Figure 4a). In addition, QTAIM analysis confirms the occurrence of BCPs and associated BPs between the bridging hydride and the two nearest gold atoms (Figure S99). As shown by the NOCV method, this interaction corresponds to the donation from the

occupied σ(B–H) MO to the σ*(Au–Au) MO with a weak yet noticeable stabilizing energy ΔE_{orb} = -8.6 kcal/mol (Figure 4b). For a more complete description of the main orbital interactions in **4**, see the supporting information (Figure S100).

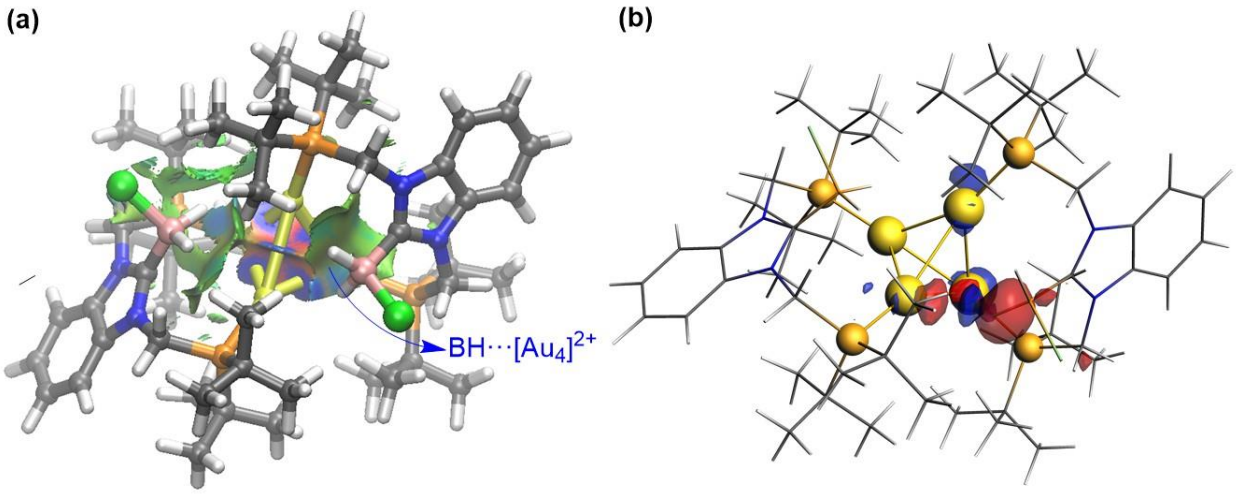

Figure 4. (a) Contour plots of the reduced density gradient isosurfaces (density cutoff of 0.04 a.u.) for compound **4**. (b) Plot of the deformation density of the pairwise orbital interactions involving the σ(B–H)→σ*(Au–Au) interaction. The color code of the charge flow is red → blue.

The mechanism of the formation of **4** was also investigated to assess the role of the new ligand platform and in particular of the central NHC-BH_3 moiety. More generally, such investigation could improve the understanding of Au nanoparticle nucleation processes, since Au nanoparticles can be generated from borohydride and even NHC-BH_3 reductants.[72-73] The formation of **4** was first followed by NMR analyses at room temperature in CD_2Cl_2. In these conditions, $^{31}P\{^1H\}$ NMR spectrum recorded after 5 min shows the complete disappearance of complex **3** and the presence of the two major triplets characterizing complex **4**. In addition, three other sets of two triplets are observed in the same area (122 to 111 ppm) which disappeared within 3 h, to the benefit of the signals of complex **4**, as the only signature observed besides a small singlet at 79.9 ppm,

unidentified so far (Figure S90). The sets of triplets likely correspond to other Au_4 clusters, given the similarities of these signals with complex **4**, both in terms of chemical shifts in ^{31}P and ^{1}H NMR spectra and in terms of multiplicity of the phosphorus nuclei. We assumed that the BH_2Cl fragment may adopt different conformations toward the Au_4 core, leading to different conformers of **4**. In agreement with this assumption, DFT calculations located another conformer lying only 0.8 kcal/mol higher in energy than **4**. In this new conformer **4-iso** (Figure S98), the B-Cl bond points toward Au-Au bonds for each ligand. In line with this assumption, ROESY experiment showed that the two inequivalent methylene-phosphine buttresses of complex **4** are in dynamic exchange with each other. This suggests an easy rotation around the B–C bond, facilitated by the weak interaction between the borane fragment and the Au_4 core (Figures S39-41).

The initial elementary step of the reaction is presumed to be the chloride abstraction by $GaCl_3$. After this step, our calculations pointed to the energetically accessible cationic dinuclear **(μ-Cl)Au_2^+** and also to the parent **(μ-H)Au_2^+** (Scheme 3). The reaction was then investigated at a lower temperature, in order to identify possible intermediates occurring before the formation of **4**. Solutions of both reagents were cooled and mixed in an NMR tube at 193 K. Four singlet signals were observed in $^{31}P\{^{1}H\}$ NMR spectrum at 193 K in the range of 82.0 to 72.0 ppm along with a minor signal corresponding to complex **3**. While the mixture did not evolve at this temperature or below, raising the temperature to 223 K led to signal broadening. After 50 minutes at 223 K, the temperature was lowered back to 183 K. The signals sharpened and only two remained at 74.9 and 78.7 ppm. The former signal at 74.9 ppm is related to a triplet in ^{1}H NMR spectrum at 6.62 ppm ($^{2}J_{P\text{-}H}$ = 92.4 Hz), which resolves into a singlet upon selective ^{31}P decoupling (Figure S95). These features are indicative of a proton coupling with two phosphorus signals that we attributed to the **(μ-H)Au_2^+** compound with a calculated $\delta_{P(calc)}$ of 76.4 ppm close to the experimental value. The

methylene signals associated with this compound are observed along with the signal for the BH_2Cl fragment at 3.9 ppm ($\delta_{H(calc)}$ = 4.4 ppm) in ^1H NMR analysis. Very few $[L_n(\mu\text{-}H)Au]_2$ systems have been reported in the literature and bridging hydrides were not always directly observed.[74] While bridging hydrides were characterized between 0.42 and -1.95 ppm in $[NHC(\mu\text{-}H)Au]_2$ complexes,[75-76] a broader range at lower field between 2.83 ($^2J_{P\text{-}H}$ = 90.9 Hz) and 8.29 ($^2J_{P\text{-}H}$ = 49 Hz) was observed in case of $[(PR_3)_n(\mu\text{-}H)Au]_2$ complexes (n = 1 or 2).[77-79]

The ^{31}P chemical shift of **(μ-Cl)Au$_2^+$** species was calculated to be 78.9 ppm (Scheme 3). By comparison, the signal detected at 78.7 ppm could thus be the signature of this species, although the signals observed initially at 72.1 and 82.0 ppm could also correspond to the bridged **(μ-Cl)Au$_2^+$** complex.

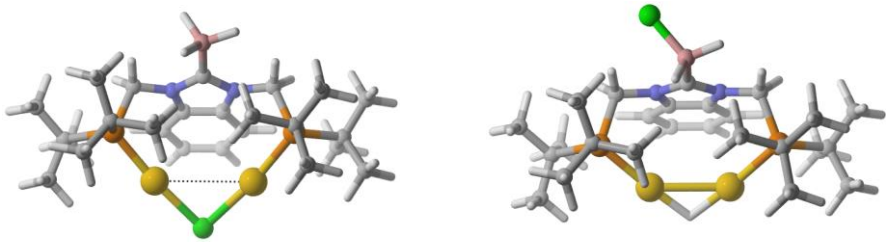

	(μ-Cl)Au$_2^+$	**(μ-H)Au$_2^+$**
E_{rel}	0.0 kcal/mol	+6.2 kcal/mol
δ_P(calc)	av. 78.9 (81.3, 76.6)	av. 76.4 (77.7, 75.1)
δ_P(exp)	78.7	74.9
δ_H(exp)	-	6.61 (t, $^2J_{P\text{-}H}$ = 92.4 Hz, μ-H), 3.9 (br, BH_2Cl)

Scheme 3. Intermediates **(μ-Cl)Au$_2^+$** and **(μ-H)Au$_2^+$**. Selected computed bond lengths [Å]: **(μ-Cl)Au$_2^+$** Au-Au 3.467, Au-Cl 2.429, Au-HB 4.938; **(μ-H)Au$_2^+$** Au-Au 2.758, Au-H 1.772, Au-HB 4.670.

When the temperature of the solution was raised to room temperature, these signals disappeared to the benefit of the cluster **4** as the major compound, suggesting that **(μ-H)Au$_2^+$** complex is an intermediate in the reaction. Since no other intermediate could be observed during the temperature

rise, the last steps involved in the formation of **4** remain to be deciphered. While further investigations will be necessary to disclose these steps, the reductive elimination of H_2 from a putative $Au_4(H)_2$ cluster obtained from dimerization of **(μ-H)Au$_2^+$** is ruled out i) by our calculations showing that the addition of H_2 to the final Au_4 complex **4** does not lead to any minimum and ii) by the observation of H_2 early on at low temperature along with **(μ-Cl)Au$_2^+$** and **(μ-H)Au$_2^+$** complexes and prior to the observation of any Au_4 cluster.

Although complex **4** proved to be sensitive toward air and light, it was stable enough for reactivity studies. The addition of 2 equivalents of $GaCl_3$ to the isolated tetragold complex **4** led to the clear formation of complex **5** (Scheme 4), which could not be isolated, but was *in situ* characterized. In the $^{31}P\{^1H\}$ NMR spectrum two triplets were observed at 125.2 and 122.4 ppm ($^3J_{P\text{-}P}$ = 24.5 Hz), indicating that the Au_4 structure was conserved, and in the $^{11}B\{^1H\}$ NMR spectrum, by a singlet at -29.4 ppm. These key signals, very similar to those in **4**, suggest minimal structural changes. A tentative structure of complex **5** is depicted in Scheme 2. We propose that the additional $GaCl_3$ interacts with the chlorine atom of each BH_2Cl moiety forming a donor-acceptor $BCl\rightarrow GaCl_3$ complex. In agreement with this hypothesis, this structure was located as a minimum on the potential energy surface by DFT calculations (Figure S98), which indicate that its formation is strongly exothermic (**4** + 2 $GaCl_3$ → **5**; ΔE = -60.5 kcal/mol).

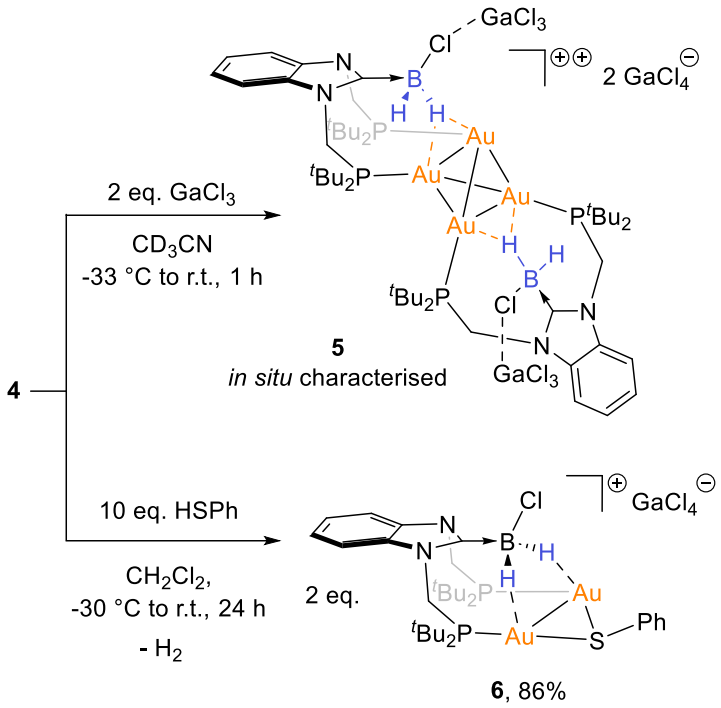

Scheme 4. Synthesis of compounds **5** and **6**.

Complex **4** was also reacted with thiophenol given the importance of thiol in gold surface chemistry.[80-82] A clean reaction is observed *in situ* leading to the isolation of complex **6** in 86% yield upon H_2 loss. The complex was characterized in solution by a singlet at 77.1 ppm in $^{31}P\{^1H\}$ analysis and at -30.2 ppm in $^{11}B\{^1H\}$ NMR analysis. Single crystals suitable for X-Ray diffraction analysis were obtained from a mixture of CH_2Cl_2 and Et_2O at low temperature. The solid state analysis showed that complex **6** is a bimetallic complex featuring a (μ-S(Ph))Au_2 core stabilized by one bisphosphine-carbene borane ligand (Figure 5a). The formation of this species is also computed to be strongly exothermic according to our DFT calculations (**4** + 2 PhSH → 2 **6** + H_2; ΔE = -44.4 kcal/mol). The gold metal centers of complex **4** have thus been re-oxidized formally by 0.5 e- to Au(I) in complex **6** (computed Au-charge of +0.24). This oxidation of a molecular gold cluster by a thiol upon loss of dihydrogen was observed once[83] and is related to the reaction of thiol with Au surfaces,[80-81, 84] while other (μ-S)Au_2 complexes were obtained by other routes.[74]

Interestingly, the BH_2Cl fragment is interacting with the Au centers through two hydrogen-gold interactions as shown by Au1···H1A 2.80(5) Å and Au2···H1B 2.70(5) Å distances at the upper limit of the sum of van der Waals radii (2.86 Å).[65] BCP (and BP) were indeed found between the B-H and gold atoms and the interaction is described by the NBO method as the donation from the doubly-occupied σ(B–H) MO to the empty σ*(Au–P) MO, with a stabilization energy value of -2.1 kcal/mol.

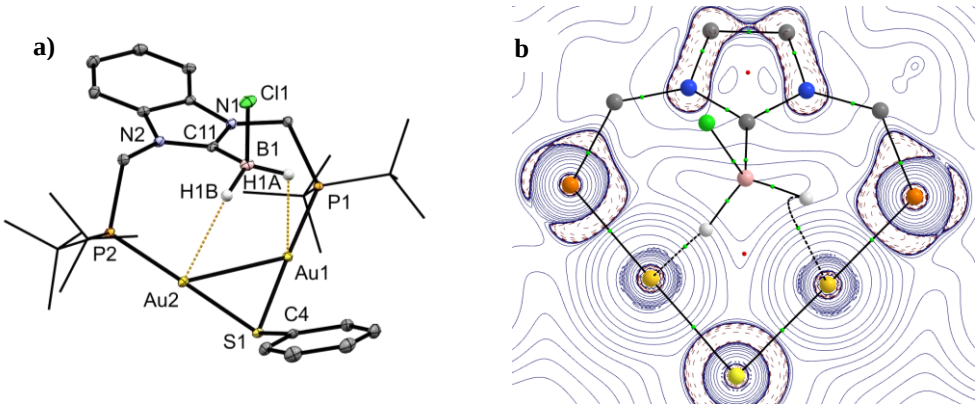

Figure 5. a) Structure of compound **6**. Thermal ellipsoids drawn at 30% probability. $GaCl_4$ anion and hydrogen atoms are omitted for clarity, except hydrides on boron which were located in the difference Fourier map and refined freely without constraints. Selected bond lengths [Å] and angles [°]: B1-C11 1.610(4), B1-H1A 1.10(5), B1-H1B 1.12(5), B1-Cl1 1.929(4), Au1-P1 2.2689(7), Au2-P2 2.2658(7), Au1-Au2 3.1263(2), Au1-S1 2.3275(7), Au2-S1 2.3291(7), Au1···H1A 2.80(5), Au2···H1B 2.70(5), Au1-S1-Au2 84.34(2), P1-Au1-S1 176.74(2), P2-Au2-S1 178.79(3); **b)** Contour map of Laplacian function ($\nabla^2\rho$) of compound **2** with relevant bond paths (black dashed line) and Bond Critical Points (BCPs, green spheres).

CONCLUSION

In conclusion, we have developed a new ligand platform that supports bimetallic structures and features a central NHC-borane moiety able to bridge gold centers with different coordination

modes. This versatile coordination behavior likely results from the weak nature of the borane-digold interaction and the easy rotation around the NHC-B bond. Moreover, the borane moiety was shown to participate in the reductive elimination of H_2 to form a Au_4 cluster that was re-oxidized upon thiol reaction. These results further expand the coordination chemistry and the reactivity of NHC-borane compounds.[40-41, 43-44] On-going investigations are directed at exploiting the rich chemistry associated with NHC-borane compounds and at expanding the coordination study to other transition metals.

AUTHOR INFORMATION

Corresponding Author

Israel Fernández - Departamento de Química Orgánica I and Centro de Innovación en Química Avanzada (ORFEO—CINQA), Facultad de Ciencias Químicas, Universidad Complutense de Madrid 28040 Madrid (Spain); Email: israel@quim.ucm.es

Sébastien Bontemps - LCC-CNRS, Université de Toulouse, CNRS, 205 route de Narbonne, 31077 Toulouse Cedex 04, France; Email: sebastien.bontemps@lcc-toulouse.fr

Author

Aurèle Camy - LCC-CNRS, Université de Toulouse, CNRS, 205 route de Narbonne, 31077 Toulouse Cedex 04, France

Laure Vendier - LCC-CNRS, Université de Toulouse, CNRS, 205 route de Narbonne, 31077 Toulouse Cedex 04, France

Christian Bijani - LCC-CNRS, Université de Toulouse, CNRS, 205 route de Narbonne, 31077 Toulouse Cedex 04, France

Author Contributions

The manuscript was written through contributions of all authors. All authors have given approval to the final version of the manuscript.

ASSOCIATED CONTENT

Supporting Information.

The supporting information are available free of charge. It includes experimental details, compounds synthesis and characterization and DFT method.

ACKNOWLEDGMENT

AC and SB thank the CNRS and the French Ministry for financial support. IF thanks financial support from the Spanish MCIN/AEI/10.13039/501100011033 (Grants PID2019-106184GB-I00 and RED2018-102387-T). For the purpose of Open Access, a CC-BY public copyright license has been applied by the authors to the present document and will be applied to all subsequent versions up to the Author Accepted Manuscript arising from this submission.

REFERENCES

1. Sinhababu, S.; Lakliang, Y.; Mankad, N. P.; Recent advances in cooperative activation of CO_2 and N_2O by bimetallic coordination complexes or binuclear reaction pathways, *Dalton Trans.* **2022**, *51*, 6129-6147.
2. Navarro, M.; Moreno, J. J.; Perez-Jimenez, M.; Campos, J.; Small Molecule Activation with Bimetallic Systems: a Landscape of Cooperative Reactivity, *Chem. Comm.* **2022**, *58*, 11220-11235.
3. Wang, Q.; Brooks, S. H.; Liu, T.; Tomson, N. C.; Tuning metal–metal interactions for cooperative small molecule activation, *Chem. Comm.* **2021**, *57*, 2839-2853.
4. Campos, J.; Bimetallic cooperation across the periodic table, *Nat. Rev. Chem.* **2020**, *4*, 696-702.
5. Berry, J. F.; Thomas, C. M.; Multimetallic complexes: synthesis and applications, *Dalton Trans.* **2017**, *46*, 5472-5473.
6. Čorić, I.; Holland, P. L.; Insight into the Iron–Molybdenum Cofactor of Nitrogenase from Synthetic Iron Complexes with Sulfur, Carbon, and Hydride Ligands, *J. Am. Chem. Soc.* **2016**, *138*, 7200-7211.
7. Buchwalter, P.; Rosé, J.; Braunstein, P.; Multimetallic Catalysis Based on Heterometallic Complexes and Clusters, *Chem. Rev.* **2015**, *115*, 28-126.
8. Park, J.; Hong, S.; Cooperative bimetallic catalysis in asymmetric transformations, *Chem. Soc. Rev.* **2012**, *41*, 6931-6943.

9. Rutz, P. M.; Grunenberg, J.; Kleeberg, C.; Unsymmetrical Diborane(4) as a Precursor to PBP Boryl Pincer Complexes: Synthesis and Cu(I) and Pt(II) PBP Complexes with Unusual Structural Features, *Organometallics* **2022**, *41*, 3044–3054.
10. Arnett, C. H.; Agapie, T.; Activation of an Open Shell, Carbyne-Bridged Diiron Complex Toward Binding of Dinitrogen, *J. Am. Chem. Soc.* **2020**, *142*, 10059-10068.
11. Esmieu, C.; Orio, M.; Le Pape, L.; Lebrun, C.; Pécaut, J.; Ménage, S.; Torelli, S.; Redox-Innocent Metal-Assisted Cleavage of S–S Bond in a Disulfide-Containing Ligand, *Inorg. Chem.* **2016**, *55*, 6208–6217.
12. Lin, T.-P.; Peters, J. C.; Boryl–Metal Bonds Facilitate Cobalt/Nickel-Catalyzed Olefin Hydrogenation, *J. Am. Chem. Soc.* **2014**, *136*, 13672-13683.
13. Esmieu, C.; Orio, M.; Torelli, S.; Le Pape, L.; Pecaut, J.; Lebrun, C.; Menage, S.; N_2O reduction at a dissymmetric {Cu_2S}-containing mixed-valent center, *Chem. Sci.* **2014**, *5*, 4774-4784.
14. Lin, Y.-W.; Rational Design of Artificial Metalloproteins and Metalloenzymes with Metal Clusters, *Molecules* **2019**, *24*, 2743.
15. Weigand, W.; Schollhammer, P., In *Bioinspired Catalysis: Metal-Sulfur Complexes*, Wiley, Ed. Weinheim, 2014.
16. Hohenberger, J.; Ray, K.; Meyer, K.; The biology and chemistry of high-valent iron–oxo and iron–nitrido complexes, *Nat. Commun.* **2012**, *3*, 720.
17. Spatzal, T.; Aksoyoglu, M.; Zhang, L.; Andrade, S. L. A.; Schleicher, E.; Weber, S.; Rees, D. C.; Einsle, O.; Evidence for Interstitial Carbon in Nitrogenase FeMo Cofactor, *Science* **2011**, *334*, 940-940.
18. Lancaster, K. M.; Roemelt, M.; Ettenhuber, P.; Hu, Y.; Ribbe, M. W.; Neese, F.; Bergmann, U.; DeBeer, S.; X-ray Emission Spectroscopy Evidences a Central Carbon in the Nitrogenase Iron-Molybdenum Cofactor, *Science* **2011**, *334*, 974-977.
19. Védrine, J. C.; Metal Oxides in Heterogeneous Oxidation Catalysis: State of the Art and Challenges for a More Sustainable World, *ChemSusChem* **2019**, *12*, 577-588.
20. Xiao, Y.; Hwang, J.-Y.; Sun, Y.-K.; Transition metal carbide-based materials: synthesis and applications in electrochemical energy storage, *J. Mater. Chem. A* **2016**, *4*, 10379-10393.
21. Roy, S.; Zhang, X.; Puthirath, A. B.; Meiyazhagan, A.; Bhattacharyya, S.; Rahman, M. M.; Babu, G.; Susarla, S.; Saju, S. K.; Tran, M. K.; Sassi, L. M.; Saadi, M. A. S. R.; Lai, J.; Sahin, O.; Sajadi, S. M.; Dharmarajan, B.; Salpekar, D.; Chakingal, N.; Baburaj, A.; Shuai, X.; Adumbumkulath, A.; Miller, K. A.; Gayle, J. M.; Ajnsztajn, A.; Prasankumar, T.; Harikrishnan, V. V. J.; Ojha, V.; Kannan, H.; Khater, A. Z.; Zhu, Z.; Iyengar, S. A.; Autreto, P. A. d. S.; Oliveira, E. F.; Gao, G.; Birdwell, A. G.; Neupane, M. R.; Ivanov, T. G.; Taha-Tijerina, J.; Yadav, R. M.; Arepalli, S.; Vajtai, R.; Ajayan, P. M.; Structure, Properties and Applications of Two-Dimensional Hexagonal Boron Nitride, *Advanced Materials* **2021**, *33*, 2101589.
22. Li, Q.; Kolluru, V. S. C.; Rahn, M. S.; Schwenker, E.; Li, S.; Hennig, R. G.; Darancet, P.; Chan, M. K. Y.; Hersam, M. C.; Synthesis of borophane polymorphs through hydrogenation of borophene, *Science* **2021**, *371*, 1143-1148.
23. Muzyka, K.; Sun, J.; Fereja, T. H.; Lan, Y.; Zhang, W.; Xu, G.; Boron-doped diamond: current progress and challenges in view of electroanalytical applications, *Analytical Methods* **2019**, *11*, 397-414.
24. Goettel, J. T.; Braunschweig, H.; Recent advances in boron-centered ligands and their transition metal complexes, *Coord. Chem. Rev.* **2019**, *380*, 184-200.
25. Saha, K.; Ghosh, S.; Hydroboration reactions using transition metal borane and borate complexes: an overview, *Dalton Trans.* **2022**, *51*, 2631-2640.
26. Pettinari, C., *Scorpionates II: Chelating Borate Ligands*. Imperial College Press: England, 2008.
27. Trofimenko, S., *Scorpionates—The Coordination Chemistry of Polypyrazolylborate Ligands*. Imperial College Press: England, 1999.
28. Hill, A. F.; Owen, G. R.; White, A. J. P.; Williams, D. J.; The sting of the scorpion: a metallaboratrane, *Angew. Chem. Int. Ed.* **1999**, *38*, 2759-2761.
29. Amgoune, A.; Bourissou, D.; [sigma]-Acceptor, Z-type ligands for transition metals, *Chem. Comm.* **2011**, *47*, 859-871.
30. Bouhadir, G.; Amgoune, A.; Bourissou, D., Chapter 1 - Phosphine-Boranes and Related Ambiphilic Compounds: Synthesis, Structure, and Coordination to Transition Metals. In *Adv. Organomet. Chem.*, Anthony, F. H.; Mark, J. F., Eds. Academic Press: 2010; Vol. Volume 58, pp 1-107.
31. Bontemps, S.; Gornitzka, H.; Bouhadir, G.; Miqueu, K.; Bourissou, D.; Rhodium(I) complexes of a PBP ambiphilic ligand: evidence for a metal -> borane interaction, *Angew. Chem. Int. Ed.* **2006**, *45*, 1611-1614.
32. Bontemps, S.; Bouhadir, G.; Miqueu, K.; Bourissou, D.; On the Versatile and Unusual Coordination Behavior of Ambiphilic Ligands o-$R_2P(Ph)BR'_2$, *J. Am. Chem. Soc.* **2006**, *128*, 12056-12057.

33. Kaur, U.; Saha, K.; Gayen, S.; Ghosh, S.; Contemporary developments in transition metal boryl complexes: An overview, *Coord. Chem. Rev.* **2021**, *446*, 214106.
34. Irvine, G. J.; Lesley, M. J. G.; Marder, T. B.; Norman, N. C.; Rice, C. R.; Robins, E. G.; Roper, W. R.; Whittell, G. R.; Wright, L. J.; Transition Metal-Boryl Compounds: Synthesis, Reactivity, and Structure, *Chem. Rev.* **1998**, *98*, 2685-2722.
35. Braunschweig, H.; Dewhurst, R. D.; Gessner, V. H.; Transition metal borylene complexes, *Chem. Soc. Rev.* **2013**, *42*, 3197-3208.
36. Braunschweig, H.; Radacki, K.; Rais, D.; Seeler, F.; Boron in the coordination spheres of three transition-metal atoms: syntheses and structures of metalloborylenes stabilized by a transition-metal base, *Angew. Chem. Int. Ed.* **2006**, *45*, 1066-1069.
37. Segawa, Y.; Yamashita, M.; Nozaki, K.; Syntheses of PBP Pincer Iridium Complexes: A Supporting Boryl Ligand, *J. Am. Chem. Soc.* **2009**, *131*, 9201-9203.
38. Segawa, Y.; Yamashita, M.; Nozaki, K.; Diphenylphosphino- or Dicyclohexylphosphino-Tethered Boryl Pincer Ligands: Syntheses of PBP Iridium(III) Complexes and Their Conversion to Iridium−Ethylene Complexes, *Organometallics* **2009**, *28*, 6234-6242.
39. Tanoue, K.; Yamashita, M.; Synthesis of Pincer Iridium Complexes Bearing a Boron Atom and iPr-Substituted Phosphorus Atoms: Application to Catalytic Transfer Dehydrogenation of Alkanes, *Organometallics* **2015**, *34*, 4011-4017.
40. Curran, D. P.; Solovyev, A.; Makhlouf Brahmi, M.; Fensterbank, L.; Malacria, M.; Lacôte, E.; Synthesis and Reactions of N-Heterocyclic Carbene Boranes, *Angew. Chem. Int. Ed.* **2011**, *50*, 10294-10317.
41. Taniguchi, T.; Advances in chemistry of N-heterocyclic carbene boryl radicals, *Chem. Soc. Rev.* **2021**, *50*, 8995-9021.
42. Bissinger, P.; Braunschweig, H.; Kupfer, T.; Radacki, K.; Monoborane NHC Adducts in the Coordination Sphere of Transition Metals, *Organometallics* **2010**, *29*, 3987-3990.
43. Hui, Z.; Watanabe, T.; Tobita, H.; Synthesis of Base-Stabilized Hydrido(hydroborylene)tungsten Complexes and Their Reactions with Terminal Alkynes To Give η3-Boraallyl Complexes, *Organometallics* **2017**, *36*, 4816-4824.
44. Bissinger, P.; Braunschweig, H.; Damme, A.; Dewhurst, R. D.; Kraft, K.; Kramer, T.; Radacki, K.; Base-Stabilized Boryl and Cationic Haloborylene Complexes of Iron, *Chem. Eur. J.* **2013**, *19*, 13402-13407.
45. Bissinger, P.; Braunschweig, H.; Damme, A.; Kupfer, T.; Radacki, K.; An Electron-Precise, Tetrahedral μ3 Boride Complex, *Angew. Chem. Int. Ed.* **2013**, *52*, 7038-7041.
46. Böser, R.; Haufe, L. C.; Freytag, M.; Jones, P. G.; Hörner, G.; Frank, R.; Completing the series of boron-nucleophilic cyanoborates: boryl anions of type NHC–B(CN)2−, *Chem. Sci.* **2017**, *8*, 6274-6280.
47. Arrowsmith, M.; Auerhammer, D.; Bertermann, R.; Braunschweig, H.; Celik, M. A.; Erdmannsdörfer, J.; Krummenacher, I.; Kupfer, T.; From Borane to Borylene without Reduction: Ambiphilic Behavior of a Monovalent Silylisonitrile Boron Species, *Angew. Chem. Int. Ed.* **2017**, *56*, 11263-11267.
48. Ruiz, D. A.; Ung, G.; Melaimi, M.; Bertrand, G.; Deprotonation of a Borohydride: Synthesis of a Carbene-Stabilized Boryl Anion, *Angew. Chem. Int. Ed.* **2013**, *52*, 7590-7592.
49. Matoba, K.; Eizawa, A.; Nishimura, S.; Arashiba, K.; Nakajima, K.; Nishibayashi, Y.; Practical Synthesis of a PCP-Type Pincer Ligand and Its Metal Complexes, *Synthesis* **2018**, *50*, 1015-1019.
50. Eizawa, A.; Arashiba, K.; Tanaka, H.; Kuriyama, S.; Matsuo, Y.; Nakajima, K.; Yoshizawa, K.; Nishibayashi, Y.; Remarkable catalytic activity of dinitrogen-bridged dimolybdenum complexes bearing NHC-based PCP-pincer ligands toward nitrogen fixation, *Nat. Commun.* **2017**, *8*, 14874.
51. One of these six molecules is depicted in Figure 1. It was chosen as the molecule featuring an average carbene-boron bond of 1.605(5) Å (C-B bonds range from 1.603(5) to 1.607(6) Å).
52. Custelcean, R.; Jackson, J. E.; Dihydrogen Bonding: Structures, Energetics, and Dynamics, *Chem. Rev.* **2001**, *101*, 1963-1980.
53. Padilla-Martińez, I. I.; Rosalez-Hoz, M. D. J.; Tlahuext, H.; Camacho-Camacho, C.; Ariza-Castolo, A.; Contreras, R.; Azolylborane adducts. Structural and conformational analysis by x-ray diffraction and NMR. Protic-hydric (C-$H^{\delta+}\cdots^{\delta-}$H-B) and Protic-Fluoride (C-$H^{\delta+}\cdots^{\delta-}$F-B) interactions, *Chem. Ber.* **1996**, *129*, 441-449.
54. Crabtree, R. H.; Recent advances in hydrogen bonding studies involving metal hydrides, *J. Organomet. Chem.* **1998**, *557*, 111-115.
55. Ramnial, T.; Jong, H.; McKenzie, I. D.; Jennings, M.; Clyburne, J. A. C.; An imidazol-2-ylidene borane complex exhibiting inter-molecular [C–$H^{\delta+}\cdots H^{\delta-}$–B] dihydrogen bonds, *Chem. Comm.* **2003**, 1722-1723.
56. Klooster, W. T.; Koetzle, T. F.; Siegbahn, P. E. M.; Richardson, T. B.; Crabtree, R. H.; Study of the N−H···H−B Dihydrogen Bond Including the Crystal Structure of BH_3NH_3 by Neutron Diffraction, *J. Am. Chem. Soc.* **1999**, *121*, 6337-6343.

57. With the silver salts $AgB(C_6F_5)_4$ or $AgSbF_6$, compound **4** was generated within a mixture of unidentified products, while the addition of $AgBF_4$ or 2 equivalents of $GaCl_3$ led to the formation of a black precipitate.
58. Nguyen, T.-A.; Daiann Sosa Carrizo, E.; Cattey, H.; Fleurat-Lessard, P.; Roger, J.; Hierso, J.-C.; Tetranuclear Dicationic Aurophilic Gold(I) Catalysts in Enyne Cycloisomerization: Cooperativity for a Dramatic Shift in Selectivity, *Chem. Eur. J.* **2022**, *28*, e202200769.
59. Schmidbaur, H.; Hamel, A.; Mitzel, N. W.; Schier, A.; Nogai, S.; Cluster self-assembly of di[gold(I)]halonium cations, *Proc. Natl. Acad. Sci.* **2002**, *99*, 4916-4921.
60. Calhorda, M. J.; Crespo, O.; Gimeno, M. C.; Jones, P. G.; Laguna, A.; López-de-Luzuriaga, J. M.; Perez, J. L.; Ramón, M. A.; Veiros, L. F.; Synthesis, Structure, Luminescence, and Theoretical Studies of Tetranuclear Gold Clusters with Phosphinocarborane Ligands, *Inorg. Chem.* **2000**, *39*, 4280-4285.
61. Crespo, O.; Gimeno, M. C.; Jones, P. G.; Laguna, A.; Villacampa, M. D.; Small Gold Clusters with Carborane Ligands: Synthesis and Structural Characterization of the Novel Compound $[Au_4\{(PPh_2)_2C_2B_9H_{10}\}_2(AsPh_3)_2]$, *Angew. Chem. Int. Ed.* **1997**, *36*, 993-995.
62. Yang, Y.; Sharp, P. R.; New Gold Clusters $[Au_8L_6](BF_4)_2$ and $[(AuL)_4](BF_4)_2$ (L = P(mesityl)$_3$), *J. Am. Chem. Soc.* **1994**, *116*, 6983-6984.
63. Zeller, E.; Beruda, H.; Schmidbaur, H.; Tetrahedral gold cluster $[Au_4]^{2+}$: crystal structure of $\{[(tert\text{-}Bu)_3PAu]_4\}^{2+}(BF_4^-)_2.2CHCl_3$, *Inorg. Chem.* **1993**, *32*, 3203-3204.
64. Demartin, F.; Manassero, M.; Naldini, L.; Ruggeri, R.; Sansoni, M.; Synthesis and X-ray characterization of an iodine-bridged tetranuclear gold cluster, di-μ-iodo-tetrakis(triphenylphosphine)-tetrahedro-tetragold, *J. Chem. Soc., Chem. Commun.* **1981**, 222-223.
65. Rigoulet, M.; Massou, S.; Sosa Carrizo, E. D.; Mallet-Ladeira, S.; Amgoune, A.; Miqueu, K.; Bourissou, D.; Evidence for genuine hydrogen bonding in gold(I) complexes, *Proc. Natl. Acad. Sci.* **2019**, *116*, 46-51.
66. Patel, D. V.; Kreisel, K. A.; Yap, G. P. A.; Rabinovich, D.; Gold(I) tris(mercaptoimidazolyl)borate chemistry: Synthesis and molecular structure of the first trinuclear TmR complex of a transition metal, *Inorg. Chem. Commun.* **2006**, *9*, 748-750.
67. Patel, D. V.; Mihalcik, D. J.; Kreisel, K. A.; Yap, G. P. A.; Zakharov, L. N.; Kassel, W. S.; Rheingold, A. L.; Rabinovich, D.; Tris(mercaptoimidazolyl)borate complexes of the coinage metals: syntheses and molecular structures of the first gold compounds and related copper and silver derivatives, *Dalton Trans.* **2005**, 2410-2416.
68. Hata, M.; Kautz, J. A.; Lu, X. L.; McGrath, T. D.; Stone, F. G. A.; Revisiting $[Mn(CO)_3(\eta^5\text{-nido-}7,8\text{-}C_2B_9H_{11})]$-, the Dicarbollide Analogue of $[(\eta^5\text{-}C_5H_5)Mn(CO)_3]$: Reactivity Studies Leading to Boron Atom Functionalization, *Organometallics* **2004**, *23*, 3590-3602.
69. Jeffery, J. C.; Jelliss, P. A.; Stone, F. G. A.; Synthesis and crystal structures of the gold–carbaborane complexes $[9\text{-exo-}\{Au(PPh_3)\}\text{-}9\text{-}(\mu\text{-}H)\text{-}10\text{-endo-}\{Au(PPh_3)\}7,8\text{-}Me_2\text{-nido-}7,8\text{-}C_2B_9H_8]$ and $[10\text{-exo-}\{Au_2(PPh_3)_2\}\text{-}10\text{-endo-}\{Au(PPh_3)\}\text{-}7,8\text{-}Me_2\text{-nido-}7,8\text{-}C_2B_9H_8]$, *J. Chem. Soc., Dalton Trans.* **1994**, 25-32.
70. Carr, N.; Gimeno, M. C.; Goldberg, J. E.; Pilotti, M. U.; Stone, F. G. A.; Topaloğlu, I.; Chemistry of polynuclear metal complexes with bridging carbene or carbyne ligands. Part 100. Synthesis of mixed-metal compounds via the salts $[NEt_4][Rh(CO)L(\eta^5\text{-}C_2B_9H_9R_2)]$(L = PPh_3, R = H; L = CO, R = Me); crystal structures of the complexes $[WRhAu(\mu\text{-}CC_6H_4Me\text{-}4)(CO)_3(PPh_3)(\eta\text{-}C_5H_5)(\eta^5\text{-}C_2B_9H11)]$ and $[WRh_2Au_2(\mu_3\text{-}CC_6H_4Me\text{-}4)(CO)_6(\eta\text{-}C_5H_5)(\eta^5\text{-}C_2B_9H_9Me_2)_2]\cdot 0.5CH_2Cl_2$, *J. Chem. Soc., Dalton Trans.* **1990**, 2253-2261.
71. Pyykkö, P.; Runeberg, N.; Calculated properties of the 'empty'$[AuPH_3]_4^{2+}$ and related systems: role of covalent and correlation contributions, *J. Chem. Soc., Chem. Commun.* **1993**, 1812-1813.
72. Hippolyte, L. New syntheses of N-heterocyclic carbene-stabilized gold nanoparticles. PhD, Sorbonne Université, 2018.
73. Bridonneau, N.; Hippolyte, L.; Mercier, D.; Portehault, D.; Desage-El Murr, M.; Marcus, P.; Fensterbank, L.; Chanéac, C.; Ribot, F.; N-Heterocyclic carbene-stabilized gold nanoparticles with tunable sizes, *Dalton Trans.* **2018**, *47*, 6850-6859.
74. A. C. A. Bayrakdar, T.; Scattolin, T.; Ma, X.; Nolan, S. P.; Dinuclear gold(i) complexes: from bonding to applications, *Chem. Soc. Rev.* **2020**, *49*, 7044-7100.
75. Phillips, N.; Dodson, T.; Tirfoin, R.; Bates, J. I.; Aldridge, S.; Expanded-Ring N-Heterocyclic Carbenes for the Stabilization of Highly Electrophilic Gold(I) Cations, *Chem. Eur. J.* **2014**, *20*, 16721-16731.
76. Tsui, E. Y.; Miller, P.; Sadighi, J. P.; Reactions of a stable monomeric gold(I) hydride complex, *Angew. Chem. Int. Ed.* **2008**, *47*, 8937-8940.
77. Campos, J.; Dihydrogen and Acetylene Activation by a Gold(I)/Platinum(0) Transition Metal Only Frustrated Lewis Pair, *J. Am. Chem. Soc.* **2017**, *139*, 2944-2947.
78. Harris, R. J.; Widenhoefer, R. A.; Synthesis, Structure, and Reactivity of a Gold Carbenoid Complex That Lacks Heteroatom Stabilization, *Angew. Chem. Int. Ed.* **2014**, *53*, 9369-9371.

79. Escalle, A.; Mora, G.; Gagosz, F.; Mézailles, N.; Le Goff, X. F.; Jean, Y.; Le Floch, P.; Cationic Dimetallic Gold Hydride Complex Stabilized by a Xantphos-Phosphole ligand: Synthesis, X-ray Crystal Structure, and Density Functional Theory Study, *Inorg. Chem.* **2009**, *48*, 8415-8422.
80. Häkkinen, H.; The gold–sulfur interface at the nanoscale, *Nat. Chem.* **2012**, *4*, 443-455.
81. Jin, R.; Quantum sized, thiolate-protected gold nanoclusters, *Nanoscale* **2010**, *2*, 343-362.
82. Negishi, Y.; Nobusada, K.; Tsukuda, T.; Glutathione-Protected Gold Clusters Revisited: Bridging the Gap between Gold(I)−Thiolate Complexes and Thiolate-Protected Gold Nanocrystals, *J. Am. Chem. Soc.* **2005**, *127*, 5261-5270.
83. Robilotto, T. J.; Bacsa, J.; Gray, T. G.; Sadighi, J. P.; Synthesis of a Trigold Monocation: An Isolobal Analogue of $[H_3]^+$, *Angew. Chem. Int. Ed.* **2012**, *51*, 12077-12080.
84. Barngrover, B. M.; Aikens, C. M.; Oxidation of Gold Clusters by Thiols, *J. Phys. Chem. A* **2013**, *117*, 5377-5384.

Graphic for Table of Contents

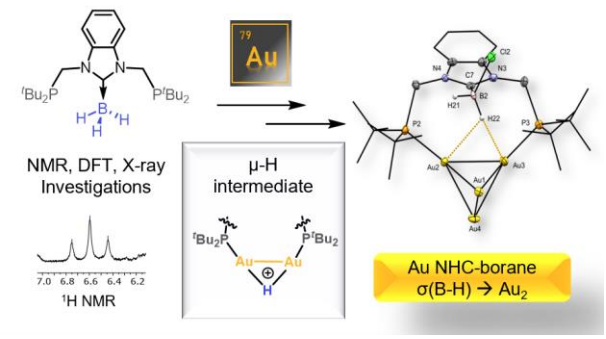

A unique bisphosphine-(NHC-borane) compound was shown to support bimetallic structure leading to the isolation of a rare Au_4 cluster with a B-H fragment bridging two Au centers.